Available online at www.sciencedirect.com
ScienceDirect
Polymer 48 (2007) 2531–2536
polymer
www.elsevier.com/locate/polymer

Polymer Communication

A new strain path to inducing phase transitions in semi-crystalline polymers

E.N. Brown [a,*], D.M. Dattelbaum [b], D.W. Brown [a], P.J. Rae [a], B. Clausen [c]

[a] *Materials Science and Technology Division, MST-8, Los Alamos National Laboratory, MS G-755, Los Alamos, NM 87545, USA*
[b] *Dynamic and Energetic Materials Division, DE-9, Los Alamos National Laboratory, Los Alamos, NM 87545, USA*
[c] *Los Alamos Neutron Science Center, LANSCE-LC, Los Alamos National Laboratory, Los Alamos, NM 87545, USA*

Received 7 February 2007; received in revised form 6 March 2007; accepted 10 March 2007
Available online 14 March 2007

Abstract

A novel application of in situ neutron diffraction under applied uniaxial strain is presented; measuring the crystalline domain evolution in a semi-crystalline polymer under bulk deformation. PTFE is shown to respond to uniaxial deformation by undergoing a crystalline phase transition that is previously believed to occur only at very high hydrostatic pressure. Discovery of this phase transition under applied uniaxial strain fundamentally changes our understanding of the deformation mechanisms in semi-crystalline polymers and how they need to be modeled. Under compression parallel to the basal plane normal (i.e., parallel to the molecular axis) the modulus is $\sim 1000\times$ bulk dominated by intra-polymer chain compression, providing experimental validation of theoretical predictions. Deformation parallel to the pyramidal plane normal exhibits both axial and transverse strains of the opposite sign as the applied load, suggesting that the crystalline lattice is accommodating deformation by shearing along the prismatic planes.
Published by Elsevier Ltd.

Keywords: Neutron diffraction; Phase transition; Polytetrafluoroethylene

1. Introduction

We present a novel application of in situ neutron diffraction under applied uniaxial strain to obtain nascent measurements of the crystalline domain evolution in a semi-crystalline polymer under bulk deformation. This powerful technique enables the measurement of the crystalline lattice strains for unique orientations of the crystalline domain relative to the far-field applied uniaxial stress ranging from prismatic plane normal (i.e., perpendicular to the molecular axis), through pyramidal plane normal, to basal plane normal (i.e., parallel to the molecular axis) within the semi-crystalline structure. To the authors' knowledge this represents the first experimental validation of theoretical predictions of polymer chain elastic response for this class of materials. Moreover, we show that in addition to the classically reported phase transitions in semi-crystalline polymers induced by hydrostatic pressure [1], the same phase transition can be achieved with much lower levels of uniaxial stress. This suggests the occurrence of a deviatoric driven phase transition, i.e., a martensitic transition. Discovery of this phase transition under applied uniaxial strain fundamentally changes our understanding of the deformation mechanisms in semi-crystalline polymers and how they need to be modeled. In the current work measurements are presented for polytetrafluoroethylene (PTFE), which is chosen for the absence of hydrogen that limits bulk diffraction acquisition in most polymers. In addition to raising the broad implications of strain induced phase transitions in the semi-crystalline polymers, this work shows that the PTFE temperature–pressure phase diagram accepted for over 50 years [2–4] is insufficient, requiring the addition of deviatoric stress dependence.

The temperature–pressure phase behavior of crystalline polytetrafluoroethylene (PTFE) (see Fig. 1a) has been extensively reported in the literature. The room temperature crystalline structure of PTFE (phase IV [3]) only exists over a narrow range of temperatures at atmospheric pressure with crystalline

* Corresponding author. Tel.: +15056670799; fax: +15056672185.
E-mail address: en_brown@lanl.gov (E.N. Brown).

0032-3861/$ - see front matter Published by Elsevier Ltd.
doi:10.1016/j.polymer.2007.03.031

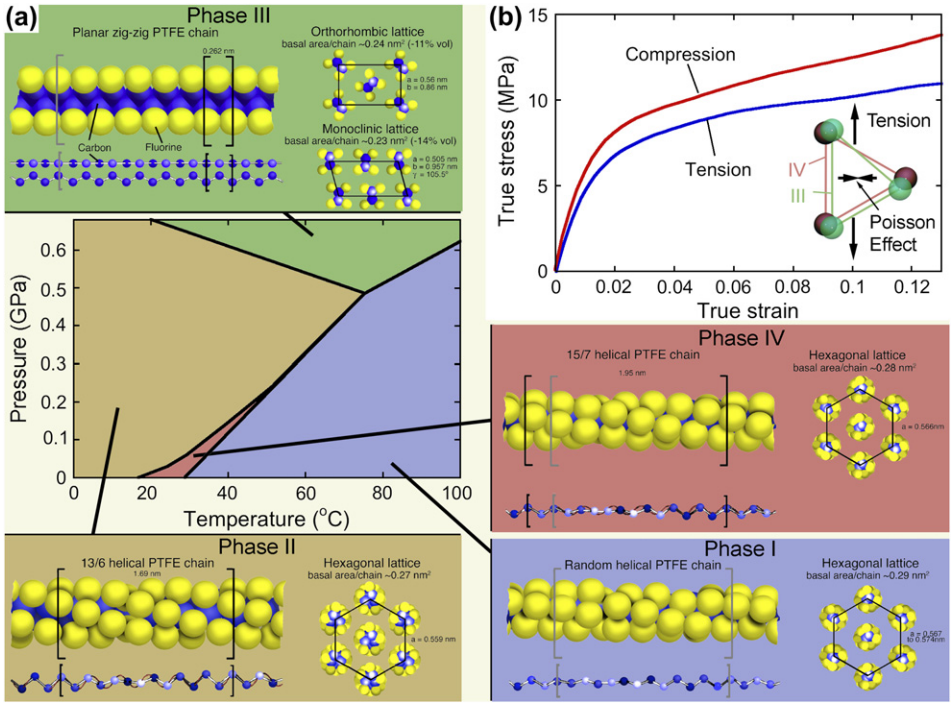

Fig. 1. Hydrostatic and uniaxial PTFE structural responses. (a) Temperature–pressure phase behavior of crystalline PTFE with the inter- and intra-polymer chain crystalline structures. (b) Bulk stress–strain response of PTFE at ambient temperature and pressure.

transitioning to phase II below 19 °C [3] and phase I above 30 °C [5]. A high-pressure phase is present above ~0.65 GPa at room temperature (phase III) [1]. The macroscopic tensile and compressive responses (see Fig. 1b) have also been extensively reported [6,7]. Up to this point, these studies reported that phase transitions were only dependent on temperature and pressure, with no effect from tension or compression. Here we show that tension and compression actually activate crystalline phase transitions at much lower stress levels.

2. Materials and methods

The pedigreed[1] PTFE polymer investigated in the current work was manufactured from PTFE 7C molding powder acquired from DuPont. Billets measuring 600 × 600 × 65 mm were pressed and sintered by Balfor Industries (NY) following ASTM D 4894-98a—an initial pressure of 3.45 MPa was applied, which was ramped to 34.5 MPa at 3–5 MPa/min, the pressed billet was sintered by an accurately controlled thermal profile of 36 °C/h to 300 °C, held for 6 h, 36 °C/h to 357 °C, held for 6 h, cooled to room temperature at 36 °C/h—resulting in a crystallinity of approximately 38% (by DSC [6]). The equivalent orthogonal diffraction patterns presented in this work suggest a random texture of the crystalline domains. Samples were machined such that the primary direction of the applied far-field stress was in the in-plane direction of the billet, while ensuring a nominal temperature rise to prevent changes in the material crystallinity. For tension measurements an ASTM D638 Type I specimen was employed with a nominal thickness of 8 mm. For compression measurements were performed on right cylinders 20 mm tall by 10 mm diameter. The bulk stress and strain responses were measured with a 100 kN load cell and knife-edge extensometer, respectively.

Two compressive and one tensile experiments were performed at room temperature using the Spectrometer for MAterials Research at Temperature and Stress (SMARTS) diffractometer at the Los Alamos Neutron Science CEnter (LANSCE) [16]. While SMARTS has enabled new fundamental understandings on metallic materials [7,18], the current work represents its first application to polymeric materials. The application of neutron diffraction to PTFE, a polymer that does not contain any hydrogen, enables measurements through specimens of ~10 mm thick.

SMARTS is a time-of-flight diffractometer using a pulsed neutron source with a range of energies. The instrument has two detector banks consisting of 196 ^{3}He filled tubes, which are located at 1.5 m from the sample. The banks are situated at ±90° to the incident neutron beam and the load frame is located at 45° to the incident neutron beam. This enables the sample to be oriented such that diffraction data can simultaneously be acquired for the atomic crystalline planes normal to the direction of applied load interrogating the relative motion of these planes parallel to direction of the applied load and crystalline plane parallel to the direction of applied load interrogating the relative motion of these planes normal to direction of the applied load. The strains calculated from these

[1] The pedigree indicates that the chemistry, manufacturing method, and material history were carefully controlled and documented. The material's pedigree reported in the current work is consistent with several previous works by the authors [6–15].

two displacement data sets are referred to as being in the axial and transverse directions, respectively, as illustrated schematically in Fig. 2a–d insets. The data were fitted using the General Structure Analysis System (GSAS) [19] on a peak-by-peak basis. Lattice spacing, d_{hkl}, for each diffraction peak with Miller indices, hkl, was determined via Bragg's law $\lambda_{hkl} = 2d_{hkl} \sin\theta$, where λ_{hkl} is the wavelength associated with the hkl reflection at a fixed angle of diffraction, $2\theta = 90°$. Changes in d-spacings are used as internal "directional" strain gages. Samples were loaded under constant engineering strain rate of $10^{-4}\ s^{-1}$. Constant strain conditions were held during diffraction measurements with an acquisition time of ~1 h. Extensive description of the facilities has been reported in the literature [16–18]. The two compressive tests performed exhibited excellent repeatability with both the bulk far-field stress–strain responses and the crystalline lattice strain

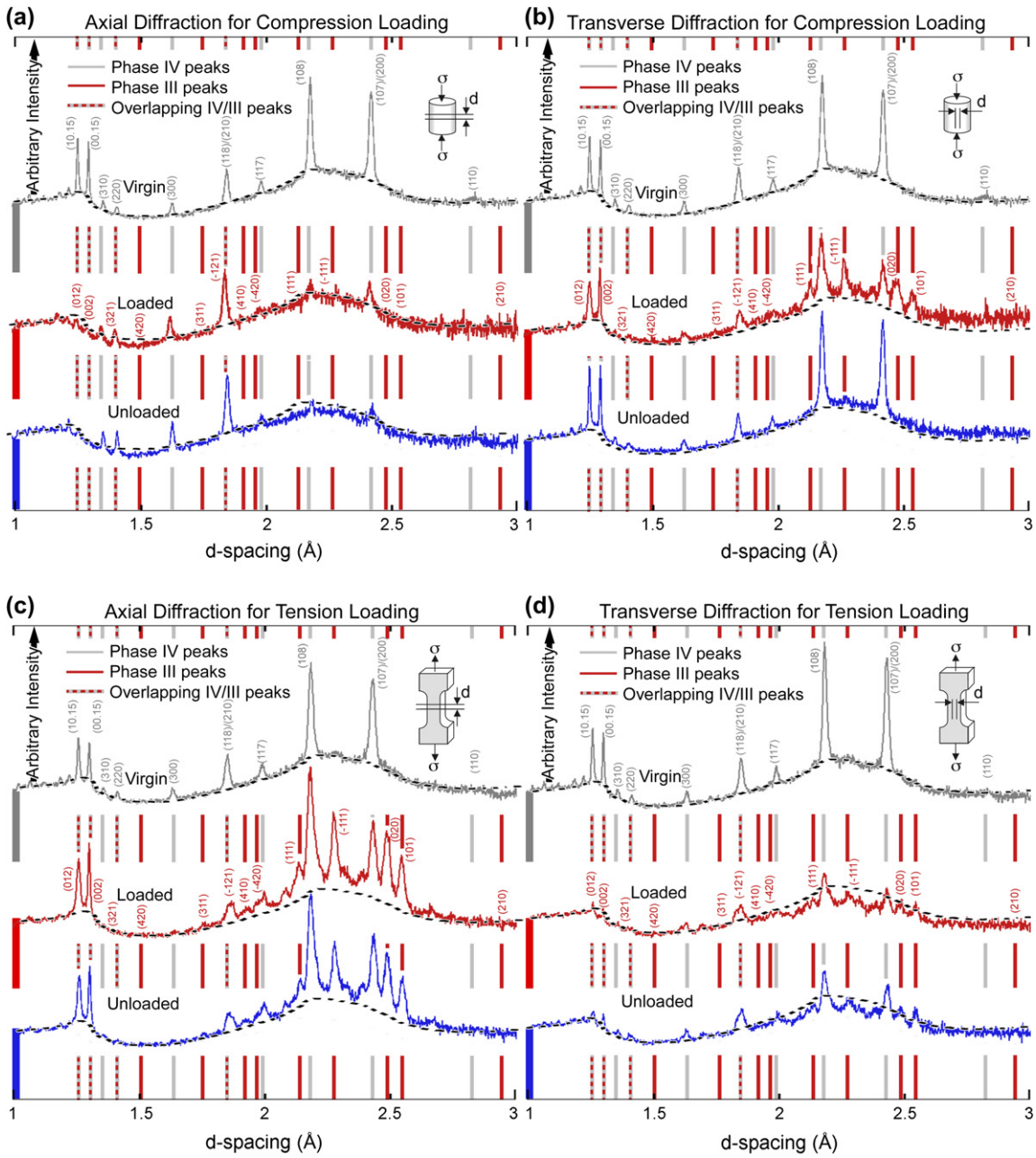

Fig. 2. PTFE d-spacing evolution under uniaxial deformation at ambient temperature and pressure. (a–d) Diffraction patterns indicate crystalline structure for compressive loading in the axial and transverse directions and tensile loading in the axial and transverse directions, respectively, (insets) as illustrated schematically for each direction of applied load and d-spacing measurement direction. Data presented for the virgin, loaded to 12% strain, and unloaded state. Light lines (|) indicate peak assignments for phase IV and dark lines (|) indicate peak assignments for phase III. The dashed lines (- -) indicate the amorphous background in the virgin state. The IV → III* transition is greatest in the direction of maximum tensile strain. For 12% compressive strain in the transverse direction where the Poisson's strain is tensile conversion from IV to III* is 25–33% and largely reversible. For 12% tensile strain in the axial direction conversion from IV to III* is 50–80% and is only partially reversible. In both cases IV → III* conversion continues with additional applied strain.

measurements for all of the crystalline lattice orientations agreeing for repeated experiments within the resolution of the experimental and analysis techniques.

3. Results and discussions

The peak locations and relative intensities of virgin zero-stress state PTFE at ambient temperature and pressure are given in Table 1a. The neutron peaks measured on bulk PTFE (see Fig. 2) correspond well with those reported from X-ray studies on undeformed PTFE powders, filaments and thin films [20–23]. Axial and transverse diffraction patterns are shown in Fig. 2 for compression and tension. The four patterns in the virgin zero-stress state agree in terms of amorphous background, peak positions, and intensity indicating initial random texture. Near 2.3 Å the amorphous background increases above the virgin condition in the transverse direction for compressive loading at 12% strain (Fig. 2b) and axial direction for tensile loading (Fig. 2c) while it decreases in the other directions. However, many of the peaks corresponding to the phase IV structure decrease significantly in intensity, while a new set of peaks is observed to grow in. These newly observed peaks are in excellent agreement with the peak assignments for the monoclinic structure of phase III [1] (Table 1b). The reported peak values for the new phase III peak under uniaxial stress are the average of the peak positions for tension and compression from both the axial and transverse diffraction patterns. It is worth noting that in some cases peak locations for phases IV and III overlap, as reported in Table 1. This is the case for convoluted peak of (210) and (118) in phase IV, which overlaps the (−121) peak in phase III. Overall this peak appears to increase in intensity during deformation, however this is expected to be an interplay between the in-growth of the (−121) peak superimposed on the out-growth of the (210) and (118) peaks. The in-growth of phase III, decrease in phase IV, and change in background are observed to occur ranked from strongest to weakest under (i) tensile loading in the axial detector direction, (ii) compressive loading in the transverse detector direction, (iii) tensile loading in the transverse detector direction, and (iv) compressive loading in the axial detector direction. Under compressive loading in the axial detector direction the in-growth of phase III and change in background are almost negligible, requiring close investigation to be noticed. This suggests a dominance of tensile strains in the observed transitions, i.e., the strongest effect is in the loading direction for an applied tensile load and the second strongest is in the transverse direction for an applied compressive load due to the Poisson's effect.

Upon unloading, the amorphous background and reverse phase transition from phase III back to phase IV exhibit mixed levels of recovery. The degree of recovery rank from most to least under (i) compressive loading in the transverse detector direction which exhibits almost full recovery, (ii) tensile loading in the transverse detector direction, (iii) compressive loading in the axial detector direction, and (iv) tensile loading in the axial detector direction. It is worth noting that upon unloading following applied strain levels in the plastic regime, PTFE retains significant residual strain. This residual strain alone indicates a lack of recovery of the polymer structure. Moreover, given the heterogeneous structure of semi-crystalline PTFE this residual strain will likely to have associated residual strains, which could further inhibit recovery. The bulk residual strain from tensile loading is observed to be greater under tension than compression, which supports the greater degree of reversibility in the case of compression. Additionally, the residual strain is greater in the axial direction where the strain is applied directly than in the transverse direction where the strain is applied second order via the Poisson's effect. This supports the observation for both tension and compression that recovery is greater in the transverse direction than in the axial direction.

The four phase III* peaks with the highest intensities—(020), (101), (111), and (111)—have a significant inter-polymer chain stress component. Since the stiffest intra-polymer chain, i.e., within the polymer chain along background, has

Table 1
(a) Crystalline lattice constants for phase IV PTFE at ambient conditions and (b) comparison of literature crystalline lattice constants for phase III PTFE at high pressure and new peaks observed at ambient temperature and pressure under uniaxial stress

(a) (*hkl*)	Phase IV measured *d*-space (Å) at zero stress	Relative intensity
100	4.902	Off range
110	2.822	W
200	2.423	Under 107
107	2.424	VS
108	2.178	VS
117	1.986	M
210	1.847	S
118	1.845	Under 210
300	1.631	M
220	1.411	M
310	1.357	M
00.15	1.299	S
10.15	1.257	S

(b) (*hkl*)	Phase III literature *d*-space (Å) at 1.2 GPa hydrostatic [1]	Measured *d*-space (Å) under uniaxial stress	Relative intensity
010	4.89	Off range	
210	2.97	2.985	W
101	2.52	2.541	VS
020	2.45	2.482	VS
−111	2.31	2.272	VS
111	2.17	2.130	S
−420	1.94	1.945	VW
410	1.90	1.895	VW
−121	1.84	Under IV 210	S
311	1.75	1.754	M
420	1.48	1.484	W
321	1.42	Under IV 220	M
002	1.31	Under IV 00.15	S
012	1.28	Under IV 10.15	S

Off range indicates that the *d*-spacing is greater than the 4 Å upper limit of SMARTS. Peak intensity based on the area between the Gaussian–Lorentzian peak shape and the local linearly fit background is qualitatively reported as very weak (VW), weak (W), medium (M), strong (S), or very strong (VS).

been shown to be ~100× higher than inter-chain, it is expected that the phase transition will be driven by the inter-chain deformation. In both phases IV and III three nearest neighbor polymer chains form the apexes of a triangle: equilateral for phase IV and acute scalene for phase III. Deformation across an equilateral triangle along any line other than the perpendicular bisector will result in an acute scalene (Fig. 1b inset), while deformation along the perpendicular bisector will mathematically generate an isosceles triangle. However, instability from the Poisson's effect bringing together the polymer chains at the apexes perpendicular to the stress will again drive the formation of an acute scalene structure. Since phase III is the lowest energy stable conformation of PTFE for this structure, it is perhaps intuitive that an applied uniaxial strain breaking the hexagonal symmetry would adopt the phase III* structure.

Fig. 3 shows representative crystallographic lattice responses to uniaxial compressive loading corresponding to macroscopic loading (Fig. 1b). In the elastic regime prior to bulk yielding for the case of loading parallel to the prismatic plane normal (310), the crystalline lattice deforms according to classic continuum mechanics with the axial and transverse strains follow Hooke's law and Poisson's response, respectively. The elastic response in the loading direction exhibits a modulus ~10× bulk (bulk ≅ 0.6 GPa) [6]. It is dominated by inter-polymer chain compression that only requires driving against the relatively weak Van der Waals' forces. Under compression parallel to the basal plane normal (00.15) the modulus is ~1000× bulk dominated by intra-polymer chain compression, corresponding to the theoretical value for a PTFE chain modulus of 220.5 GPa [24] within the experimental error. To the authors' knowledge, the current work is the first experimental validation of this theoretical work. Deformation parallel to the pyramidal plane normal (108) exhibits both axial and transverse strains of the opposite sign as the applied load, suggesting that the crystalline lattice is accommodating deformation by shearing along the prismatic planes, supporting the proposal of Flack [25]. The results of two repeated compression experiments exhibited excellent repeatability at both the macroscopic (mm) and crystallographic lattice (Å) length scales. Results from the tensile experiment exhibit the same three mechanisms as observed in compression.

PTFE is shown to respond to uniaxial deformation by undergoing a crystalline phase transition previously believed to occur only at very high hydrostatic pressure. We have demonstrated that in situ neutron diffraction can be applied to probe the crystalline domains in a bulk semi-crystalline polymer. It holds promise for future applications to additional fluoro- and low-hydrogen polymers, polymer matrix composites, and nascent biomimetic and nano-structured polymers. We have presented heterogeneous strains in the crystalline domains and the evolution of the structure. The strongest changes in structure are shown to occur in the direction of the maximum tensile stress component, i.e., in the loading direction for an applied tensile load and in the transverse direction for an applied compressive load due to the Poisson's effect. Combining the current results on the crystalline strains with the recent work of Poulsen et al. [26] for amorphous strains will provide even more complete insight into the behavior of semi-crystalline polymers. These results will aid the development of predictive physically based models for the semi-crystalline polymer structure–property relationship similar to current polycrystalline models for metals [27].

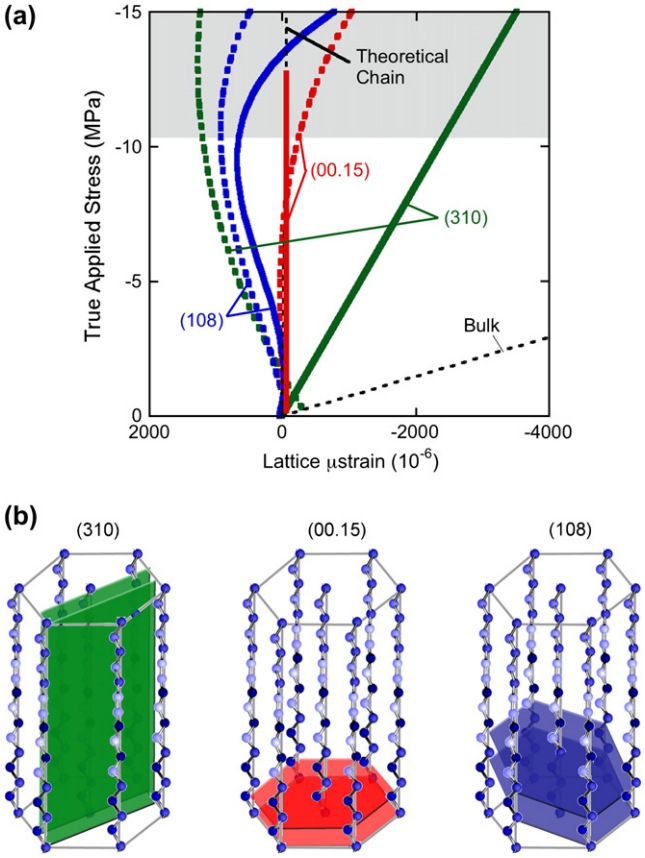

Fig. 3. PTFE crystallographic lattice responses to uniaxial compressive loading. (a) Lattice stress–strain responses for representative prismatic (310), basal (00.15), and pyramidal (108) orientations. The solid lines (—) are for the axial direction and the dashed lines (- -) are for the transverse directions. The bulk and theoretical chain responses are shown for reference. Below yield each curve is fit through 23 data points collected on two samples. The disparity between the crystalline and bulk responses arises from the very compliant amorphous phase of the composite-like semi-crystalline structure. (b) Representative unit cells for the (310), (00.15), and (108) orientations. The *d*-spacing is the normal distance between the indicated parallel planes and the lattice strains are calculated from the change in this distance. For the axial case the load is also applied normal to these plane, whereas for the transverse case the load is being applied in the plane.

Acknowledgements

This research was supported under the auspices of the US Department of Energy operated by Los Alamos National Security LLC, and the Joint DoD/DOE Munitions Program. This work has benefited from the use of the Lujan Neutron Scattering Center at LANSCE, which is funded by the Department of

Energy's Office of Basic Energy Sciences. Los Alamos National Laboratory is operated by Los Alamos National Security LLC under DOE Contract DE-AC52-06NA25396.

References

[1] Flack HD. J Polym Sci 1972;10:1799.
[2] Rigby HA, Bunn CW. Nature 1949;164:583.
[3] Bunn CW, Howells ER. Nature 1954;174:549.
[4] Patrick CR. Nature 1958;181:698.
[5] Sperati CA. Fluorine-containing polymers, II: polytetrafluoroethylene. Fortschr Hochpolym-Forsch Bd 1961;2:465–95.
[6] Rae PJ, Dattelbaum DM. Polymer 2004;45:7615.
[7] Rae PJ, Brown EN. Polymer 2005;46:8128.
[8] Bourne NK, Gray III GT. J Appl Phys 2003;93:8966.
[9] Robbins DL, Sheffield SA, Alcon RR. In: Furnish MD, Gupta YM, Forbes JW, editors. Shock compression of condensed matter—2003. Melville, NY: American Institute of Physics; 2004. p. 675–8.
[10] Brown EN, Dattelbaum DM. Polymer 2005;46:3056.
[11] Rae PJ, Brown EN, Clements BE, Dattelbaum DM. J Appl Phys 2005;98:063521.
[12] Brown EN, Rae PJ, Gray III GT. J Phys IV 2006;134:935.
[13] Brown EN, Rae PJ, Orler EB, Gray III GT, Dattelbaum DM. Mater Sci Eng C 2006;26:1338.
[14] Brown EN, Trujillo CP, Gray III GT, Rae PJ, Bourne NK. J Appl Phys 2007;101:024916.
[15] Brown EN, Rae PJ, Liu C. Mater Sci Eng A 2007. doi:10.1016/j.msea.2006.09.125.
[16] Bourke MAM, Dunand DC, Ustundag E. Appl Phys A 2002;74:S1707.
[17] Clausen B, Lorentzen T, Bourke MAM, Daymond MR. Mater Sci Eng A 1999;259:17.
[18] Brown DW, Bourke MAM, Dunn PS, Field RD, Stout MG, Thoma DJ. Metall Mater Trans A 2001;32:2219.
[19] Von Dreele RB, Jorgensen JD, Windsor CG. J Appl Crystallogr 1982;15:581.
[20] Clark ES, Muus LT. Z Kristallogr 1962;117:119.
[21] Kimmig M, Strobl G, Stühn B. Macromolecules 1994;27:2481.
[22] Weeks JJ, Clark ES, Eby RK. Polymer 1981;22:1480.
[23] Bouznik VM, Kirik SD, Solovyov LA, Tsvetnikov AK. Powder Diffr 2004;19:219.
[24] Bartha F, Bogar F, Peeters A, Van Alsenoy C, Van Doren V. Phys Rev B 2000;62:10142.
[25] Flack HD. J Polym Sci 1974;12:81.
[26] Poulsen HP, Wert JA, Neuefeind J, Honkimaki V, Daymond M. Nature Mater 2005;4:33.
[27] Lebensohn RA, Tome CN. Acta Metall Mater 1993;41:2611.